RSC Advances

ROYAL SOCIETY OF CHEMISTRY

www.rsc.org/advances

Journal Name

ARTICLE

Carbon microspheres air electrode for rechargeable Li-O_2 battery

Wei Meng[a], Shengwei Liu[a], Lina Wen[a] and Xue Qin*[a]

Received 00th January 20xx,
Accepted 00th January 20xx

DOI: 10.1039/x0xx00000x

www.rsc.org/

The carbon microspheres (CMs) are synthesized by reflux-calcinations method showing large BET surface of 626.919 m^2 g^{-1}, typical micropore structure and good electrochemical properties. The CMs which are employed as an air cathode without the addition of any metal particles not only provide reaction sites but also act as cathode carbon support in the non-aqueous system of the Li-O_2 batteries. An initial discharge capacity of 12081.0 mAh g^{-1} could be obtained at 200mA g^{-1}. Little capacity loss is shown after 20 full discharge / charge cycles under a current density of 300 mA g^{-1}. 60 cycles of continuous discharge and charge are achieved with no capacity loss with a cut-off capacity of 1000 mAh g^{-1}, at 200 mA g^{-1}. The reversible formation is clearly revealed by CV curves.

1. Introduction

Rechargeable Li-O_2 batteries, due to their substantially higher energy density than conventional lithium-ion batteries, have a big potential for the application of future electrochemical power sources [1-4]. But so far, the Li-O_2 batteries have not been put into application in our daily life because many factors influence the Li-O_2 batteries' practical realization, including the poor cycling stability, the poor rate capability, the short calendar life and the low round-trip efficiency [5].

To solve the above problems, various approaches have been developed to address these problems, including the use of a stable electrode, trace amounts of electrolyte additives [6-8], redox mediators in electrolytes and oxygen electrodes with optimized microstructures [9,10]. Among them, the cathode material is the most important one. As a vital area, where Li-O_2 heterogeneous reactions happen and the discharge products are hosted, the polarization of the cathode catalyst could be a big obstacle to the electrochemical characteristics of Li-O_2 batteries [11-14]. The key charge / discharge reaction take place at the cathode electrode is $2Li^{+}+2e^{-}+O_2 \leftrightarrow Li_2O_2$ (E=2.96 V) [15-17]. Li_2O_2, the discharged product, is insoluble and it will be stored in the pores of the cathodes [18]. A cathode material with enough micropores to store the insoluble Li_2O_2 as well as good activity on the oxygen reduction reaction (ORR) and the oxygen evolution reaction (OER) is suitable for being used as cathode material of the Li-O_2 batteries [16]. Until now, various carbon materials have been widely studied for those advantages [11,20], such as carbon nanotubes (CNTs), super P, carbon nanofiber, graphene, ketjen black and carbon nanoballs (CNBs)

[a] Department of chemistry, School of Science, Tianjin University, and Collaborative Innovation Center of Chemical Science and Engineering (Tianjin), Tianjin 300072, China.

[12, 21-24]. Aiming to achieve promising electrochemical performance, many researchers have been investigating to combine transition metal oxides (MnxOy and perovskites) with those carbon materials for applications to Li-O_2 batteries. However, those conventional carbon composites have suffered from multiple drawbacks, such as complex synthesizing process, high cost as well as capacity fading on cycling which result from load shedding during charging and discharging process. Today, extensive studies have been conducted in search for non-precious-metal materials. A particularly promising example was the development of the naostructured multihole metal-free carbon catalysts with analogous functions and comparable reactivity to those of conventional noble metals [25].

In this paper, the as-prepared carbon microspheres (CMs) are reported as the air cathode in the non-aqueous electrolyte of lithium bis-tri-fluoromethanesulfonyl imide (LiTFSI) in tetraethylene glycol dimethyl ether (TEGDME) system. The battery with the CMs based cathode can sustain 60 stable cycles with a cut off capacity of 1000 mAh g^{-1} at the current density of 200 mA g^{-1}. Excellent electrochemical properties are shown according to the electrochemical measurements of cyclic voltammograms (CV) and electrochemical impedance spectroscopy (EIS）

2. Experimental

2.1 Preparation of catalyst

The CMs were synthesized by the follows: (1) 5 wt% sucrose in 6 M H_2SO_4 solution was stirred and heated to reflux for 10 h, followed by being filtered and washed with deionized water and ethanol, then dried to obtain the precursor of CMs; (2) the precursor was calcined at 1000 °C for 2 h in muffle furnace and cooled to room temperature in nitrogen atmosphere; (3) the above samples were activated at 400 °C for 1 h in air to get the CMs.

2.2 Physical Characterizations of the cathode material

The morphology of the as-synthesized CMs was observed using transmission electron microscopy (TEM, Tecnai G2 F20) and scanning electron microscope (SEM, S4800). And the specific surface area of the materials was calculated using the Brunauere-Emmette-Teller (BET).

2.3 Preparation of electrode and Li-O_2 cell assembling configuration

The electrochemical behaviors were measured in Swagelok cells with a 1.0 cm^2 hole placed on the cathode which enabled the oxygen flow in. The prepared CMs were mixed with AB (acetylene black) as a conductive agent and polyvinylidene fluoride (PVDF) as a binder in N-methyl-2-pyrrolidone with a mass ratio of 70:10:20 wt% to form homogeneous slurry. With a mass loading of 1.2±0.05mg cm^{-2}, the cathode mixture was brushed onto a carbon paper（purchased from Shanghai Hesen, 0.3 mm thickness), followed by being dried at 120 °C under vacuum oven for 12h. Li foil was used as the anode and separated by poly (-tetrafluoro-ethylene) (PTFE) membrance. 1 M lithium bis-tri-fluoromethane-sulfonyl imide (LiTFSI) in tetraethylene glycol dimethyl ether (TEGDME) was used as the electrolyte. The cells were assembled in a glove box filled with high-purity argon (O_2 and H_2O < 1 ppm) and were recorded by a battery testing system (LAND CT-2001A system). Cyclic voltammetry (CV) curves are collected using Zahner Ennium electrochemical workstation.

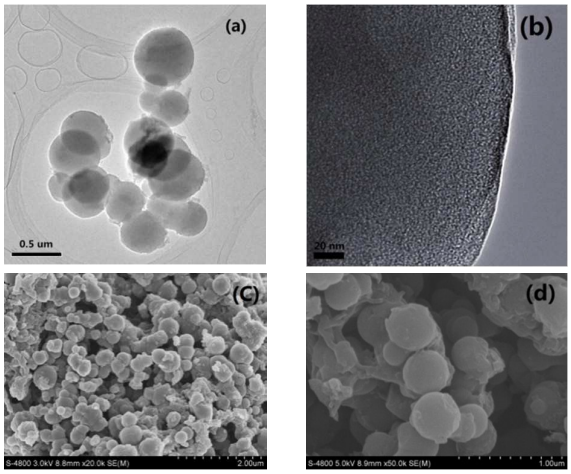

Fig. 1. TEM imagines (a) (b) and SEM imagines (c) (d) of the CMs

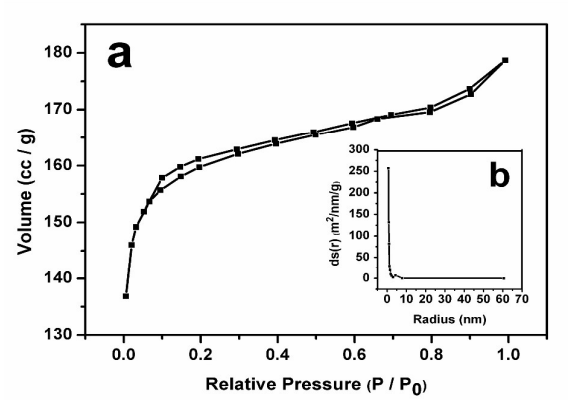

Fig. 2. N_2 adsorption-desorption isotherms curves and pore size of the CMs.

3. Results and discussion

3.1 Structure of the CMs

From the images of the TEM and SEM in Fig. 1a, Fig. 1c and d, we can see that the as-prepared CMs almost own the same diameter of 400 nm with a smooth edge. What's more, the high-magnification TEM image in Fig. 1b shows that the CMs are full of nanosized pores. Further, the N_2 adsorption / desorption isotherms reveal that the pore-size distribution is centered at 0-5 nm while relatively lower proportion peaks are centered at 9 nm, as observed in Fig. 2b. Moreover, the BET

surface area for the CMs is as high as 626.919 m^2 g^{-1}. The CMs with high surface area and nanosized pores in the mesoporous structure not only significantly allows efficient oxygen diffusion but also enhances the electrode / electrolyte contact area [26]. That is what important for being used as cathode material of the Li-O_2 battery.

3.2 Electrochemical characteristics of the Li-O_2 cells

The discharge–charge measurement was performed in the voltage range of 2.0–4.5V (vs. Li/Li^+). Both the applied current (mA g^{-1}) and achieved capacity (mAh g^{-1}) were normalized to the weight of CMs. Figure 3a shows the first six full discharge-charge curves of the battery with CMs at 200mA g^{-1}. Obviously, the battery with CMs delivered an initial discharge capacity of 12081.0 mAh g^{-1} and the discharge voltage is 2.65V. Even after six cycles, the battery can even show a discharge capacity of 5406.9 mAh g^{-1}, exhibiting huge energy potential. As the current density even increased to 300mA g^{-1} in Fig. 3b, the discharge platform showed almost no change compared with that at 100mA g^{-1}. It's worthy to note that the Li-O_2 battery can cycle up to 20 full discharge-charge cycles with less capacity loss at 300mA g^{-1}. As we known, pure carbon materials which could show such a stable full discharge-charge capacity have rarely been reported because of the accumulation of the discharge product and the instability of the electrolyte [24]. For comparison and rule out other factors in the system, we contrasted a Li-O_2 battery using pure AB as well as PVDF with mass ratio of 9:1 and determined its full discharge-charge curves. The capacity decay became obvious after the tenth cycle, as shown in Fig. 3c. We therefore conclude that the presence of the CMs can improve the capacity and cycle stability greatly. This could be attributed to the pores as well as big surface area of the CMs which can testify for storing the discharge product and enhance the reversibility of the Li-O_2 battery.

To further investigate the cyclability of the CMs based cathode, cycle performance is tested at restricted discharge-charge depth at the current density of 200 mA g^{-1}. Fig. 3d presents cycling curves, maintaining the capacity at 1000 mAh g^{-1} for both charging and discharging. The cells showed good performance over 60 cycles with stable discharge–charge voltage platforms and the corresponding profiles are depicted in Figure 3d. The CMs showed stable discharge platform at 2.60 V and low-charge voltage at 4.2 V in the first cycle. Obviously, during the initial 30 cycles, the discharge and charge platforms maintained very stable with low overpotential, indicating the excellent electrochemical activity of Li-O_2 batteries with CMs air cathode catalysts, and in the following cycles the charge potential gradually increased and reached above 4.5 V at the finishing point of the 60th charge.

The charge / discharge performance is accompanied by the accumulation and decomposition of the Li_2O_2 [29]. To further explore and gain insight into discharge and charge process, we use SEM and XRD to analyze the product during the first cycle. After discharge to 2.0V at 300 mA g^{-1}, as shown in Fig. 4b, many small particles aggregated on the surface of the spheres, which are considered to be Li_2O_2 precipitate. When the cell was recharged to 4.5V, a relatively clean cathode was observed in Fig. 4c, and almost recovered to the pristine morphology which is shown in Fig.4a. This can be further proved by XRD patterns in Fig.4d. The peaks of Li_2O_2 could be clearly observed in the discharge electrode. After the subsequent charge process, the Li_2O_2 characteristic peaks nearly disappeared, indicating good reversibility of the battery.

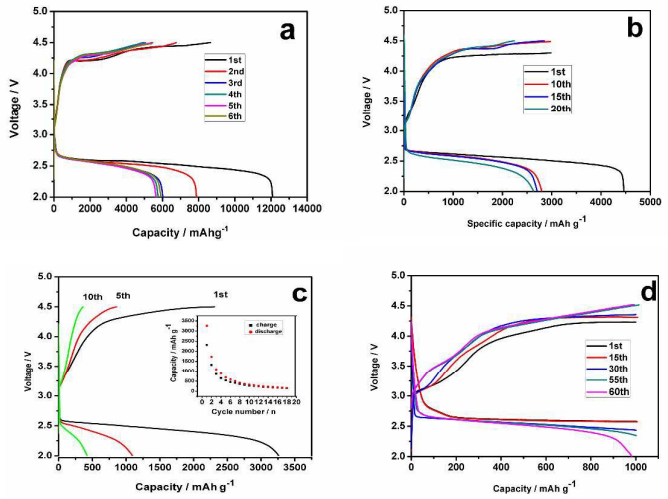

Fig.3. First six full charge-discharge curves of Li-O_2 battery with CMs cathode at 200mA g^{-1} (a), the first 20 charge-discharge curves at 300mA g^{-1} with CMs cathode (b) and pure AB (insert: capacity vs cycle number graph) (c). The cycle curves at restrict charge-discharge depth of 1000 mAh g^{-1}, at 200 mA g^{-1} (d).

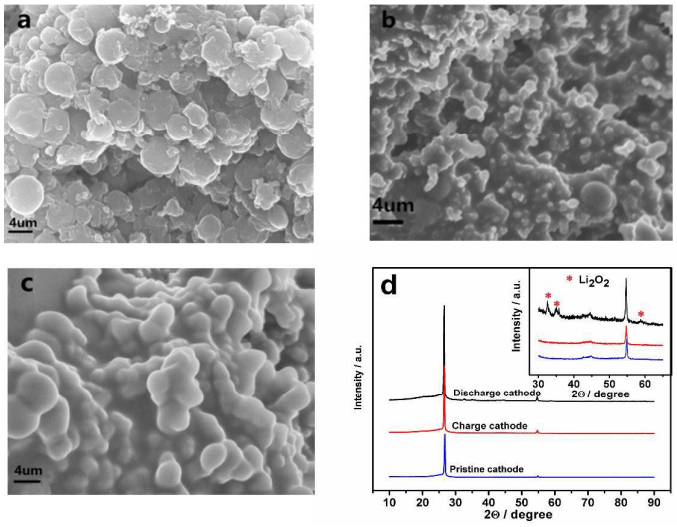

Fig. 4. SEM images of the pristine cathode (a), the discharged (b) and the recharged (c) cathode during the first cycle. XRD patters for pristine cathode, the discharge and recharged cathode during the first cycle (insert: a zoom in the diffractogram from 30–60°) (d).

In order to understand the catalytic activity of the electrodes, the cyclic voltammetry (CV) curves of the battery were tested in the voltage range of 2.4-4.8 V at a scan rate of 0.1 mV s^{-1}, which was shown in Fig. 5a. Compared with the electrode with pure AB, the cathode with CMs exhibited more apparent ORR and OER peaks and higher peak current, which

indicates higher catalytic activity for Li-O_2 batteries. Obviously, for CMs cathode, tow anodic peaks and two cathodic peaks were detected here, signifying the existence of the two electrochemical events. In the second cycle, the cathodic peak in lower potential at 3.37V was decreased being explained by the reduction of the electronic conductivity of air electrolyte, which might attribute to the incomplete decomposition of the reduction Li_2O_2 particles in the previous cycle [21]. In the Li^+ conducting electrolyte, the reduction of O_2 molecules proceeds from O_2^- (LiO_2) to O_2^{2-} (Li_2O_2) and to O^{2-} (Li_2O) [28]. The undecomposed or survived LiO_2 could further react with Li^+ and e^- to generate Li_2O_2 [13, 28]. The peak at 3.37V could be ascribed to the further reduction of LiO_2 to Li_2O_2 and the Li_2O_2 was readily reduced to Li_2O which formed the higher potential peaks at 3.62V. Notably, during the oxidation scan, the obvious oxidation peaks were well correspond with the reduction ones, which is the evidence for the good reversibility of the CMs catalyst.

Electrochemical impedance spectroscopy (EIS) measurements were carried out to compare the electrochemical performance of the CMs cathode with pure AB ones. Fig. 5b and Fig. 5c show the electrochemical impedance spectra of the CMs cathode and the bare AB ones at 298K. The impedance spectra are both composed of a semicircle corresponding to the contact resistance and charge transfer resistance, as well as a slope related to the mass diffusion within the air cathode. Fig. 4d shows the equivalent circuit of the two electrodes, where R_1, R_2, R_3, CPE2, CPE3 are denoted as solution resistance, SEI film resistance, reaction resistance, double layer capacitance, and diffusion capacitance. A constant phase element (CPE) replaces the capacitor element reasonably [26, 30]. A CPE is usually defined as $\{Y (jw)\}^{-1}$. A nonlinear, least-square fitting calculation is performed using the equivalent circuit. For CMs electrode, the R_3 and CPE2 value (T) are 0.1297 Ω·g, 1.582 F/g and bare AB electrode are 0.2598 Ω·g, 0.04214 F/g. The R_3 of the CMs electrode is lower than that of the AB ones, demonstrating that the polarizability of the CMs is lower. The value of CPE2 value is related to the true reaction areas of the electrode [26,30], so the CMs have larger reaction areas than AB. Therefore, it is concluded that the enhanced charge–discharge behaviour of CMs catalysts can be explained by the lower cell reaction resistance and the larger reaction areas.

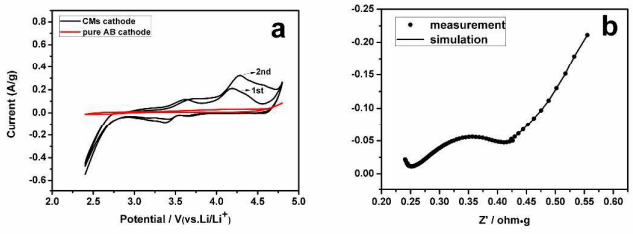

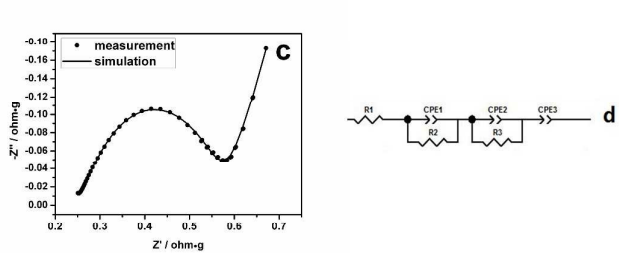

Fig. 5. CV curves of the battery with CMs cathode and pure AB cathode at the scan rate of 0.1mVs^{-1} (a), Nyquist impedance plots of the CMs (b) and pure AB (c) based battery after the initial discharge process and the corresponding equivalent circuit of the two electrode (d).

4. Conclusions

In summary, CMs which are synthesized by reflux-calcinations method have been studied for being used as air cathode in the non-aqueous Li-O_2 battery. The CMs have delivered a high initial discharge capacity of 12081.0 mAh g^{-1} at the current density of 200 mA g^{-1} and enable 60 cycles at restrict capacity depth of 1000 mAh g^{-1} at 200 mA g^{-1}. Even at 300mA g^{-1}, little capacity loss has been shown after 20 full charge-discharge cycles. The battery with CMs shows enhanced electrochemical behaviour than with pure AB during cycling. Good reversibility and mechanism for the CMs based battery have been exactly given by the CV curves.

Acknowledgements

The authors gratefully acknowledge the financial support from the Open Project of Key Lab Adv. Energy Mat. Chem. (Nankai Univ.) (KLAEMC-OP201201) partially.

Notes and references

[1] L.Y. Li, J.J. Wang, X.F. Li, J. Liu, D.S. Geng, J.L. Yang, R.Y. Li, X.L. Sun, Electrochem. Commun., 2011, **13**, 668.
[2] R. Cao, J.S. Lee, M.L. Liu, J. Cho, Adv. Energy Mater., 2012, **2** ,816.
[3] R.E. Williford, J.-G. Zhang, J. Power Sources, 2009, **194**, 1164.
[4] Q.-C. Liu, J.J. Xu, Z.W. Chang, X. B. Zhang, J. Mater. Chem. A, 2014, **2**, 6081.
[5] Z.l. Jian, P. Liu, F.J. Li, P. He, X.W. Guo, M.W. Chen, H.S. Zhou, Angew. Chem. Int. Ed., 2014, **53**, 442.
[6] N.B. Aetukuri, B.D. McCloskey, J.M. García, L.E. Krupp, V. Viswanathan, A.C. Luntz, Nat Chem, 2015, **7**, 50.
[7] S. Meini, M. Piana, N. Tsiouvaras, A. Garsuch, H.A. Gasteiger, Electrochemical and Solid-State Letters, 2012, **15**, 45.
[8] K.U. Schwenke, M. Metzger,T. Restle, M. Piana, H.A. Gasteiger, Journal of The Electrochemical Society 2015, **162**, 573.
[9] H.G. Jung, J. Hassoun, J.B. Park, Y.K. Sun, B. Scrosati, Nat. Chem., 2012, **4**, 579.
[10] J.L. Shui, F. Du, C.M. Xue, Q. Li, L.M. Dai, ACS NANO, 2014, 8, 3015.
[11] L. Qing, X. Ping, G. Wei, Adv. Mater., 2014, 26, 1378.
[12] L. Xu, J. Ma, B.H. Li, F.Y. Kang, J. Power Sources, 2014, **255**, 187.
[13] Z.Q. Peng, S.A. Freunberger, L.J. Hardwick, Y.H. Chen, V. Giordani, F. Barde, P. Novak, D. Graham, J.M. Tarascon, P.G. Bruce, Angew. Int. Ed., 2011, **50**, 6351.
[14] D.S. Kim, Y.J. Park, Electrochimica Acta, 2014, **132**, 297.
[15] N. Imanishi, O. Yamamoto, MATERIALS TODAY, 2014, **17**, 24.

[16] B.D. McCloskey, D.S. Bethune, R.M. Shelby, G. Girishkumar, A.C. Luntz, JOURNAL OF PHYSICAL CHEMISTRY LETTERS, 2011, **2**, 1161.
[17] U. Sahapatsombut, H. Cheng, K. Scott, J. Power Sources, 2014, **249**, 418.
[18] L.L. Zhang, F.F. Zhang, G. Huang, J.W. Wang, X.C. Du, Y.L. Qin, L.M. Wang, J. Power Sources, 2014, **261**, 311.
[19] Y. Chen, F.J. Li, D.-M. Tang, Z.L. Jian, C. Liu, D. Golberg, A.Yamada, H.S. Zhou, J. Mater. Chem. A, 2013, **1**, 13076.
[20] Ma. SB, Lee. DJ, Roev. V, Im. D, Doo. SD, J. Power Sources, 2013, **244**, 496.
[21] W. Xu, V.V. Viswanathan, D.Y. Wang, S.A. Towne, J. Xiao, Z.M. Nie, D.H. Hu, J.G. Zhang, J. Power Sources, 2011, **196**, 3894.
[22] H.L.Wang, Y. Yang, Y. Liang, G. Zheng, Y. Li, Y. Cui, H. Dai, Energy Environ. Sci., 2012, **5**, 7931.
[23] Yang. SB, Feng. XL, Zhi. LJ, Cao.QA, Maier. J, Mullen. K, Adv. Mater., 2010, **22**, 838.
[24] J. Kang, O.L. Li, N. Saito, J. Power Sources, 2014, **261**, 156.
[25] Y. Zheng,Y. Jiao, L. Ge, M. Jaroniec, S. Z.Qiao, Angew. Chem. Int. Ed., 2013, **52**, 3110.
[26] H.L. Gao, Z. Y. Li, X. Qin, J. Power Sources, 2014, **248**, 565.
[27] Zhang, Z., Chen, Y., Bao, J., Xie, Z., Wei, J., Zhou, Z., Part. Part. Syst. Charact. 2015
[28] C.O. Laoire, S. Mukerjee, K.M. Abraham, J. Phys. Chem. C, 2010, **114**, 9178.
[29] G.Y. Zhao, J.X. Lv, Z.M. Xu, L. Zhang, K.N. Sun, J. Power Sources, 2014, **248**, 1270.
[30] J. Højberg, B.D. McCloskey, J. Hjelm, T. Vegge, K. Johansen, P. Norby, A. C. Luntz, ACS Appl. Mater. Interfaces, 2015, **7**, 4039.